Christiane's Hair

Jacques Lévy Véhel and Franklin Mendivil

Abstract. We explore the geometric and measure-theoretic properties of a set built by stacking central Cantor sets with continuously varying scaling factors. By using self-similarity, we are able to describe its main features in a fairly complete way. We show that it is made of an uncountable number of analytic curves, compute the exact areas of the gaps of all sizes, and show that its Hausdorff and box-counting dimensions are both equal to 2. It provides a particularly good example to introduce and showcase these notions because of the beauty and simplicity of the arguments. Our derivation of explicit formulas for the areas of all of the gaps is elementary enough to be explained to first-year calculus students.

1. INTRODUCTION. Consider the beautiful and striking set illustrated below (let us call the set $\mathcal{CH}$).

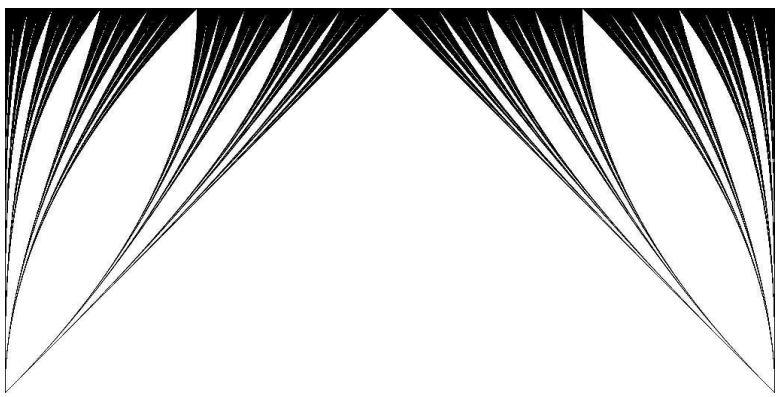

Clearly, this set has an intricate recursive (fractal) structure. In fact, it is constructed by "stacking" Cantor sets (in a way that we will describe momentarily). We can also see that $\mathcal{CH}$ is composed of uncountably many "strands." Our name for the set (and this paper) was inspired by the resemblance of $\mathcal{CH}$ to the braided hair of the first author's wife, Christiane.

Here we explore some geometric and measure-theoretic properties of this set. We hope to convince you that the elegance and simplicity of the geometrical arguments are just as striking as the set itself.

2. CONSTRUCTION OF $\mathcal{CH}$. First we must describe the construction of $\mathcal{CH}$. The basic construction is very simple. Above, we said that $\mathcal{CH}$ is composed of a "stack" of Cantor sets, so first we meditate on so-called "central" Cantor sets, with the classical Cantor set as the most famous example (also called Smith–Cantor sets, as Henry Smith had described similar sets independently of Cantor [**6**, p. 45]). The classic Cantor set is constructed by starting with the unit interval $I = [0, 1]$ and then removing the middle $1/3$ (as an open interval) to obtain the two closed intervals $I_0 = [0, 1/3]$ and $I_1 =$

http://dx.doi.org/10.4169/amer.math.monthly.120.09.771
MSC: Primary 28A80, Secondary 28A78

[2/3, 1]. Repeating for each of the closed intervals, we remove the open middle 1/3 to obtain four closed intervals $I_{00} = [0, 1/9]$, $I_{01} = [2/9, 1/3]$, $I_{10} = [2/3, 7/9]$, and $I_{11} = [8/9, 1]$. After the nth iteration, we have 2^n closed intervals of length 3^{-n}. The union of these 2^n intervals together comprise a set C_n. Noticing that $\{C_n\}$ is a nested collection of non-empty compact sets, we then see that $\mathcal{C} = \cap_n C_n$ is non-empty and compact; this is the classical Cantor set, also called the "middle 1/3-Cantor set." This construction is illustrated in Figure 1.

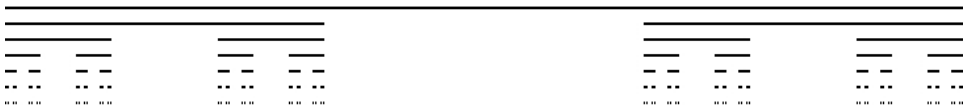

Figure 1. Iterative construction for the classical Cantor set $\mathcal{C}$

In this figure, we can see the binary structure of $\mathcal{C}$ clearly. In fact, $\mathcal{C}$ is homeomorphic to the countably infinite product of the two-point discrete space $\{0, 1\}$. We can think of a point $x \in \mathcal{C}$ as resulting from an infinite sequence of choices of *left* or *right*. Each such sequence of choices selects some nested sequence of closed intervals, one from each stage of the construction. The intersection of the resulting nested intervals is always a single point. As an example, choosing the left interval at each stage will result in the point $x = 0$.

It is simple to modify the construction of $\mathcal{C}$ where we remove some other (fixed) ratio of the length at each stage. We shall denote by $\mathcal{C}_y$ the set obtained by removing the length $1 - 2y$ in the middle of $[0, 1]$ at the first stage, where y ranges in $[0, 1/2]$ (the reason for our funny choice of $1 - 2y$ for the gap length will become evident below). At the nth stage, we have 2^{n-1} remaining closed intervals, each of length y^{n-1}, and we remove a length of $(1 - 2y)y^{n-1}$ from the middle of each interval. We build in this way a continuum of Cantor sets, where the size of the gaps at each stage decrease. When $y = 1/2$, we do not remove anything, so the resulting set is just the interval $[0, 1]$, while for $y = 0$, the resulting set is reduced to the two-point set $\{0, 1\}$. The vertical stacking of the C_y for y from 0 to 1/2 is our set $\mathcal{CH}$.

More formally,

$$\mathcal{CH} = \left\{(x, y) : x \in \mathcal{C}_y, y \in [0, 1/2]\right\} \subset [0, 1] \times [0, 1/2]. \tag{1}$$

Another, more useful way of constructing the classical Cantor $\mathcal{C}$ set is by using an Iterated Function System (IFS) [**1, 7**]. Consider the two functions

$$w_0(x) = x/3 \quad \text{and} \quad w_1(x) = x/3 + 2/3.$$

Notice that $w_0(\mathcal{C}) = \mathcal{C} \cap [0, 1/3]$ and $w_1(\mathcal{C}) = \mathcal{C} \cap [2/3, 1]$, so that

$$\mathcal{C} = w_0(\mathcal{C}) \cup w_1(\mathcal{C}), \tag{2}$$

with the union being disjoint. This *self-tiling* or *self-similarity* property uniquely defines $\mathcal{C}$ in that if $A \subset \mathbb{R}$ is any non-empty compact set with $A = w_0(A) \cup w_1(A)$, then it must be the case that $A = \mathcal{C}$. Moreover, the set-valued mapping $\hat{W}$ given by $\hat{W}(A) = w_0(A) \cup w_1(A)$ is contractive in the Hausdorff metric, and thus we have that $\hat{W}^n(A)$ converges to $\mathcal{C}$ for any non-empty compact $A \subset \mathbb{R}$. Note that Figure 1 illustrates this convergence with the initial set $A = [0, 1]$. The first line in the figure shows

$A = [0, 1]$, the second line shows $\hat{W}(A) = [0, 1/3] \cup [2/3, 1]$, the third line shows $\hat{W}^2(A) = [0, 1/9] \cup [2/9, 1/3] \cup [2/3, 7/9] \cup [8/9, 1]$, and so on.

The self-similarity and uniqueness properties of $\mathcal{C}$ also allow us to give another useful description of it. Consider the set

$$A = \left\{ \sum_{n=1}^{\infty} t_n 3^{-n} : t_n \in \{0, 2\} \right\}. \tag{3}$$

Then it is not so hard to see that

$$w_0(A) = \left\{ \sum_{n \geq 1} t_n 3^{-n} : t_1 = 0, t_n \in \{0, 2\} \text{ for } n \geq 2 \right\}$$

and

$$w_1(A) = \left\{ \sum_{n \geq 1} t_n 3^{-n} : t_1 = 2, t_n \in \{0, 2\} \text{ for } n \geq 2 \right\},$$

so $A = w_0(A) \cup w_1(A)$. However, this means that $A = \mathcal{C}$ and so (3) gives an explicit description of $\mathcal{C}$. For the more general situation below it will be useful to notice that

$$\left\{ \sum_{n=1}^{\infty} t_n 3^{-n} : t_n \in \{0, 2\} \right\} = \left\{ 2 \sum_{n \geq 1} b_n 3^{-n} : b_n \in \{0, 1\} \right\}.$$

The sets $\mathcal{C}_y$ introduced above are also obviously associated to iterated functions systems. For $y \in [0, 1/2]$, we define the two maps

$$w_0(x, y) = yx \quad \text{and} \quad w_1(x, y) = yx + (1 - y). \tag{4}$$

Thus, $y = 1/3$ yields the classical Cantor set, while $y = 1/4$ yields a middle-$1/2$ version of it.

Each $\mathcal{C}_y$ is the unique invariant set under the two maps given in (4). The entire set $\mathcal{CH}$ is invariant under these two maps as well, where we now think of these maps as $w_0, w_1 : [0, 1] \times [0, 1/2] \to [0, 1] \times [0, 1/2]$, abusing notation slightly. The reason we label the sets $\mathcal{C}_y$ is that y is the contraction factor for the IFS (4). Labeling each Cantor set in the "stack" by its central gap length would result in messier formulas for the IFS (4).

Comments. The set $\mathcal{CH}$ is a nice illustration of how the interval $[0, 1]$ has been "ripped apart" to form the classical Cantor set. We see at all the points with two binary representations, that is, all the numbers of the form $i/2^j$, that the interval $[0, 1]$ has been cut and a gap has been inserted. More specifically, a gap of length 3^{-n} has been inserted at each point of the form $i/2^n$ for $1 \leq i \leq 2^n - 1$. It is best to think of this construction in stages, as with the usual construction. First, we cut at $x = 1/2$, scale each half by a factor of $2/3$, and insert a gap of length $1/3$. The scaling preserves the total length. Then, we cut at the points that originally had coordinates $1/4$ and $3/4$ (now their coordinates have changed), scale each part by $2/3$, and insert gaps of length $1/9$. This is illustrated in $\mathcal{CH}$ where a gap originates at each dyadic point on the top line, when they are inserted.

The IFS (4) for $\mathcal{CH}$ is not contractive and has many compact invariant sets on the space $[0, 1] \times [0, 1/2]$. In fact, it has uncountably many. Simply take any closed subset $S \subset [0, 1/2]$ and obtain an invariant set of the form

$$\left\{(x, y) : x \in \mathcal{C}_y, y \in S\right\}.$$

The set $\mathcal{CH}$ is the maximal compact invariant subset of $[0, 1] \times [0, 1/2]$ in the sense that it contains any other invariant compact subset.

We make no claim to having discovered $\mathcal{CH}$. For instance, Mandelbrot's book [**10**] contains a version of it on page 81.

3. AREAS OF THE "GAPS" OF $\mathcal{CH}$. The starting point for this paper was a surprising (to us) observation about the areas of the "gaps" of $\mathcal{CH}$. In this short section we explain this pretty little geometric fact, which is simple enough that it can be explained to calculus students.

Consider the set $\mathcal{CH}$ as enclosed in the box $[0, 1] \times [0, 1/2]$. We notice that the central "gap" (or void) is a triangle with base length equal to one and height equal to $1/2$. (It is worthwhile spending a little bit of time understanding why it is actually a triangle.)

Remarkably, it is possible to **exactly** compute the areas of all the other gaps, even though their sides are complicated curves. For instance, each of the two "stage-two" gaps (the images of the central gap) have area

$$\int_{y=0}^{y=1/2} (1 - 2y)y \, dy = \frac{1}{24}.$$

How does this formula arise? We see that for any given y, the set $\mathcal{C}_y$ has a central gap of length $1 - 2y$. Because of the self-similarity of $\mathcal{C}_y$ under the two maps given in (4), the common length of the next largest gaps (one on either side of the central gap) is equal to $y(1 - 2y)$. Thus, the area of either one of these "stage-two" gaps is the integral of this length over y.

In a similar way, the "nth-stage" gaps all have area equal to

$$\int_{y=0}^{y=1/2} (1 - 2y)y^{n-1} \, dy = \frac{2^{-n}}{n(n + 1)}.$$

We can check that the sum of these areas is, in fact, equal to $1/2$, the entire area of the rectangle. Computing this sum is simple, as it is a telescoping sum:

$$\sum_{n \geq 1} 2^{n-1} \frac{2^{-n}}{n(n + 1)} = \frac{1}{2} \sum_{n \geq 1} \frac{1}{n} - \frac{1}{n + 1} = \frac{1}{2}.$$

Thus $\mathcal{CH}$ has Lebesgue measure zero.

4. EACH STRAND OF "HAIR" IS A SMOOTH CURVE. $\mathcal{CH}$ is comprised of an uncountable collection of continuous curves, each of which goes from some point on the top horizontal line down to one of the two points $(0, 0)$ or $(1, 0)$. All of the curves (the "hairs" or "strands") that you can see in the image are actually smooth, in fact polynomials (the horizontal, x, coordinate is a polynomial function of y). To understand this, just notice that each curve that bounds a "gap" is the image of one of

the two diagonal edges of the central triangle under some finite composition of the two IFS maps. We say more about this in this section.

We will prove that each strand is a C^∞ curve, and also that each strand is an analytic curve. Clearly, knowing that they are analytic curves imply that they are C^∞, so why present both proofs? We are interested in more than just arriving at the strongest results; we are mainly interested in presenting engaging mathematics, and we believe both proofs are appealing. The proof that strands are C^∞ is a good illustration of a standard technique in fractals. The argument defines an IFS on functions and their derivatives and shows that this "vector IFS" process converges uniformly, thus yielding the result. The proof that the strands are analytic uses an explicit power series representation of the strand functions. This argument also uses IFS, but in a different way.

The collection of strands is not, in fact, indexed by the points on the top line (the points in [0, 1]), but is indexed by infinite binary sequences. One clue to this is that the two sides of the central triangle both originate at $x = 1/2$. What is special about $x = 1/2$ is that it has two binary representations, so we need to consider them separately; each representation leads to its own strand. As the Cantor set has a binary structure, this is not surprising.

To describe the strands, we need to establish some notation. For any $n \in \mathbb{N}$, we set $\Sigma^n = \{0, 1\}^n$ as the space of length n binary sequences. Further, $\Sigma = \{0, 1\}^{\mathbb{N}}$, and for $\sigma \in \Sigma$ we define $\sigma^n \in \Sigma^n$ as $\sigma^n = (\sigma_1, \sigma_2, \ldots, \sigma_n)$, the truncation of σ to the first n places. Given two functions ϕ_0 and ϕ_1 and $\sigma \in \Sigma^n$, we define the nth order composition ϕ_σ by

$$\phi_\sigma := \phi_{\sigma_1} \circ \phi_{\sigma_2} \circ \cdots \circ \phi_{\sigma_n}. \tag{5}$$

The order of composition in (5) is very important. Notice the difference between

$$\phi_{\sigma^n} = \phi_{\sigma_1} \circ \phi_{\sigma_2} \circ \cdots \circ \phi_{\sigma_n}$$

and

$$\phi_{\sigma^{n+1}} = \phi_{\sigma_1} \circ \phi_{\sigma_2} \circ \cdots \circ \phi_{\sigma_n} \circ \phi_{\sigma_{n+1}}$$

for a given $\sigma \in \Sigma$. The "newest" map is applied on the "inside."

We consider everything as a function of y (since we are trying to show that all the "hairs" are smooth functions of y). Acting on a function $f : [0, 1/2] \to [0, 1]$, $x = f(y)$, we have that the two IFS maps from (4) are given as

$$\phi_0(f)(y) = yf(y) \quad \text{and} \quad \phi_1(f)(y) = yf(y) + 1 - y, \quad \text{for } y \in [0, 1/2].$$

Notice that, by the definition of ϕ_i, we have $\phi_i(f) : [0, 1/2] \to [0, 1]$ whenever $f : [0, 1/2] \to [0, 1]$. Since $y \in [0, 1/2]$, both ϕ_1 and ϕ_2 are contractions on $C[0, 1/2]$ in the uniform norm with contractivity $1/2$. Furthermore, for any $\sigma \in \Sigma^n$, the contractivity of ϕ_σ is 2^{-n}. In addition, for $\sigma \in \Sigma$ and $m > n \geq 1$, we have $|\phi_{\sigma^m}(f)(y) - \phi_{\sigma^n}(f)(y)| \leq 2^{-n}$. Thus, for any fixed $\sigma \in \Sigma$, we have that the limit

$$\mathcal{T}_\sigma(y) := \phi_\sigma(f)(y) = \lim_n \phi_{\sigma^n}(f)(y) \tag{6}$$

exists and is uniform in y (since the contraction factor is uniformly bounded in y). For the "hairs," our starting functions are $f_0(y) = 0$ for all y (the left edge) and $f_1(y) = 1$ for all y. The two edges of the central triangle are $\phi_0(f_1)(y) = y$ and $\phi_1(f_0)(y) = 1 - y$. Then the boundaries of the next gap (at "stage" 2) are the four curves:

$$\phi_0(\phi_0(f_1))(y) = y^2,$$
$$\phi_0(\phi_1(f_0))(y) = y - y^2,$$
$$\phi_1(\phi_0(f_1))(y) = y^2 + 1 - y,$$
$$\phi_1(\phi_1(f_0))(y) = 1 - y^2.$$

From these considerations, it is clear that all the boundary curves of any of the nth stage "gaps" are polynomials of degree n. The strand associated with $\sigma \in \Sigma$ is the uniform limit in (6) and is thus a continuous function. We show that all of the derivatives converge uniformly as well. To do this, just notice that

$$(\phi_0(f))'(y) = yf'(y) + f(y) \quad \text{and} \quad (\phi_1(f))'(y) = yf'(y) + f(y) - 1. \tag{7}$$

Continuing on to the second derivative, we see that

$$(\phi_0(f))''(y) = yf''(y) + 2f'(y) \quad \text{and} \quad (\phi_1(f))''(y) = yf''(y) + 2f'(y), \tag{8}$$

and the nth derivatives mappings for $n > 1$ are

$$(\phi_0(f))^{(n)}(y) = yf^{(n)}(y) + nf^{(n-1)}(y) = (\phi_1(f))^{(n)}(y). \tag{9}$$

This means that we have two linear mappings on the function value and its first n derivatives, which are given by

$$\Phi_0 \begin{pmatrix} f \\ f' \\ f'' \\ \vdots \\ f^{(n-1)} \\ f^{(n)} \end{pmatrix} = \begin{pmatrix} y & 0 & 0 & \cdots & 0 & 0 \\ 1 & y & 0 & \cdots & 0 & 0 \\ 0 & 2 & y & \cdots & 0 & 0 \\ \vdots & \vdots & \vdots & \ddots & \vdots & \vdots \\ 0 & 0 & 0 & \cdots & y & 0 \\ 0 & 0 & 0 & \cdots & n & y \end{pmatrix} \begin{pmatrix} f \\ f' \\ f'' \\ \vdots \\ f^{(n-1)} \\ f^{(n)} \end{pmatrix} \tag{10}$$

and

$$\Phi_1 \begin{pmatrix} f \\ f' \\ f'' \\ \vdots \\ f^{(n-1)} \\ f^{(n)} \end{pmatrix} = \begin{pmatrix} y & 0 & 0 & \cdots & 0 & 0 \\ 1 & y & 0 & \cdots & 0 & 0 \\ 0 & 2 & y & \cdots & 0 & 0 \\ \vdots & \vdots & \vdots & \ddots & \vdots & \vdots \\ 0 & 0 & 0 & \cdots & y & 0 \\ 0 & 0 & 0 & \cdots & n & y \end{pmatrix} \begin{pmatrix} f \\ f' \\ f'' \\ \vdots \\ f^{(n-1)} \\ f^{(n)} \end{pmatrix} + \begin{pmatrix} 1 - y \\ -1 \\ 0 \\ \vdots \\ 0 \\ 0 \end{pmatrix}. \tag{11}$$

It is clear that both Φ_0 and Φ_1 are contractive (recall $y \leq 1/2$), and thus the first n derivatives converge uniformly as well. Since this is true for any n, $\mathcal{T}_\sigma(y) = \phi_\sigma(f)(y)$ is a C^∞ function of y for any $\sigma \in \Sigma$.

We note that it is easy to show from (7) that $|\mathcal{T}'_\sigma(y)| \leq 2$ for all y and $\sigma \in \Sigma$. This fact will be important in section 5.

Thread functions are analytic. A completely different approach to the thread functions shows that these functions are, in fact, real analytic.

The idea is based on the representation given in (3) for the special case of the classical Cantor set with $y = 1/3$. For $y \in (0, 1/2]$, we claim that

$$\mathcal{C}_y = \left\{ (1-y)y^{-1} \sum_{n\geq 1} \sigma_n y^n : \sigma \in \Sigma \right\}. \tag{12}$$

We use the self-similarity of $\mathcal{C}_y$ to show this.

Let the set defined on the right-hand side of (12) be denoted by S_y. As a set of subsums of the convergent geometric series $\sum_n y^n$, S_y is a non-empty and compact set (see [**5, 8, 11**]). Furthermore,

$$\begin{aligned} w_0(S_y) &= \left\{ (1-y)y^{-1} \sum_{n\geq 1} \sigma_n y^{n+1} : \sigma \in \Sigma \right\} \\ &= \left\{ (1-y)y^{-1} \sum_{n\geq 1} \alpha_n y^n : \alpha \in \Sigma, \alpha_1 = 0 \right\}, \end{aligned}$$

and

$$\begin{aligned} w_1(S_y) &= \left\{ (1-y) + (1-y)y^{-1} \sum_{n\geq 1} \sigma_n y^{n+1} : \sigma \in \Sigma \right\} \\ &= \left\{ (1-y)yy^{-1} + (1-y)y^{-1} \sum_{n\geq 1} \sigma_n y^{n+1} : \sigma \in \Sigma \right\} \\ &= \left\{ (1-y)y^{-1} \sum_{n\geq 1} \alpha_n y^n : \alpha \in \Sigma, \alpha_1 = 1 \right\}. \end{aligned}$$

Thus $S_y = w_0(S_y) \cup w_1(S_y)$, and so $S_y = C_y$. This means that the "thread function" $\mathcal{T} : \Sigma \times [0, 1/2] \to [0, 1]$ is given by

$$\mathcal{T}_\sigma(y) = (1-y)y^{-1} \sum_{n\geq 1} \sigma_n y^n. \tag{13}$$

For a fixed $\sigma \in \Sigma$, this is a real-analytic function for $y \in (0, 1/2]$.

5. GEOMETRIC MEASURE-THEORETIC PROPERTIES OF $\mathcal{CH}$. We now turn to deeper geometric properties of $\mathcal{CH}$, in particular the Hausdorff measure and dimension and the box-counting dimension. We discuss some very basic background on these two topics. For a more complete discussion, we suggest that the reader consult the books [**3, 4, 9, 12, 13**]. In particular, chapter 3 of Falconer's book [**3**] has a very nice general discussion about dimensions. In our brief overview, we will provide some of the simpler arguments to give the reader a feel for these dimensions, but we will omit the more complicated ones to keep our discussion to a reasonable length. A full understanding of these dimensions is not necessary to appreciate our discussion, so the reader should feel safe in skipping some background details.

We start with the Hausdorff dimension, even though the box-counting dimension is more elementary. In our case, the Hausdorff dimension is easier to compute.

5.1. The Hausdorff dimension of $\mathcal{CH}$. First, we remind the reader about the definition and one or two simple properties of the Hausdorff s-dimensional measures, which we denote by h^s. We use $|A|$ for the diameter of $A \subset \mathbb{R}^d$. For $\delta > 0$, a *δ-cover of A* is a countable cover $\{U_i\}$ of A with $|U_i| \leq \delta$ for each i. Given a Borel set $A \subset \mathbb{R}^d$, we define

$$h^s_\delta(A) = \inf\left\{\sum_i |U_i|^s : \{U_i\}\ \delta\text{-cover of } A\right\} \quad \text{and} \quad h^s(A) = \lim_{\delta\to 0} h^s_\delta(A).$$

From standard results in measure theory, h^s is a Borel measure. Furthermore, it is possible to show that for integer values of n, the Hausdorff measure h^n is a constant multiple of n-dimensional Lebesgue measure. The definition of h^s is guided by the same intuition as for Lebesgue measure, but with the "size" of a "basic" set U given by $|U|^s$ (rather than its n-dimensional volume).

We see that if $s < t$, then $h^s_\delta(A) \geq \delta^{s-t} h^t_\delta(A)$. This implies that if $h^t(A) > 0$, then $h^s(A) = +\infty$. Therefore, there is a special value, denoted by $\dim_H(A)$ and called the *Hausdorff dimension of A*, such that for $0 \leq s < \dim_H(A)$ we have $h^s(A) = +\infty$, and for $s > \dim_H(A)$ we have $h^s(A) = 0$. Any $A \subset \mathbb{R}^d$ with non-empty interior has Hausdorff dimension d, so this notion agrees with our intuitive idea of dimension for nice sets. However, unlike our intuitive notion of dimension, it is certainly possible for sets to have fractional Hausdorff dimension. As an example, $\dim_H(\mathcal{C}_y) = -\ln(2)/\ln(y)$. The Hausdorff dimension is *monotone* ($A \subseteq B$ implies $\dim_H(A) \leq \dim_H(B)$) and *countably stable* ($\dim_H(\cup_i A_i) = \sup_i \dim_H(A_i)$). Sets with $0 < h^s(A) < \infty$ are called *s-sets* and have been extensively studied. In fact, any generalized Cantor set is an s-set for an appropriate dimension function [**2**].

The measure h^s has a nice behaviour under Lipschitz mappings, which will be very important for us. Let $f : \mathbb{R}^d \to \mathbb{R}^d$ be Lipschitz (that is, $\|f(x) - f(y)\| \leq K\|x - y\|$ for some constant K), then $|f(U)|^s \leq K^s|U|^s$ and thus $h^s(f(A)) \leq K^s h^s(A)$. In particular, $\dim_H(f(A)) \leq \dim_H(A)$.

$\dim_H(\mathcal{CH}) = 2$. We now show that the Hausdorff dimension of $\mathcal{CH}$ is equal to two. One interesting feature is that "locally" the Hausdorff dimension of $\mathcal{CH}$ is strictly less than two everywhere except in neighborhoods of the top line. Locally, $\mathcal{CH}$ is close to being a product of a Cantor set (in the horizontal direction) with an interval (in the vertical direction). The local geometry of $\mathcal{CH}$ varies considerably from top to bottom.

Clearly, the Hausdorff dimension of $\mathcal{CH}$ is at least one, since it contains many smooth curves any of which have dimension equal to one. We show that it is actually equal to two. For $[a, b] \subset (0, 1/2)$ let $K^b_a = ([0, 1] \times [a, b]) \cap \mathcal{CH}$. We show that $\dim_H(K^b_a) \geq 1 - \ln(2)/\ln(a)$. By 7.2 in [**3**] we know that

$$\dim_H(\mathcal{C}_a \times [a, b]) \geq \dim_H(\mathcal{C}_a) + \dim_H([a, b]) = -\ln(2)/\ln(a) + 1,$$

an intuitively plausible but nontrivial result to prove. Thus, if we can construct a Lipschitz surjection $\Phi : K^b_a \to \mathcal{C}_a \times [a, b]$, we then know that $\dim_H(K^b_a) \geq 1 - \ln(2)/\ln(a)$ as well.

Our first step is to define a family of Lipschitz surjections $\phi^\beta_\alpha : \mathcal{C}_\beta \to \mathcal{C}_\alpha$ whenever $\alpha < \beta$. We use the representation from (12) to define ϕ^β_α. Given $x \in \mathcal{C}_\beta$, there is a unique $\sigma \in \Sigma$ for which $x = (1 - \beta)\beta^{-1} \sum_n \sigma_n \beta^n$. Using this binary encoding, we define

$$\phi^\beta_\alpha(x) = (1 - \alpha)\alpha^{-1} \sum_n \sigma_n \alpha^n. \tag{14}$$

Notice that x and $\phi_\alpha^\beta(x)$ are on the same strand. Geometrically, we can think that ϕ_α^β "slides" the point x down the strand from $\mathcal{C}_\beta$ to $\mathcal{C}_\alpha$. We say "down", since $\mathcal{C}_\beta$ is higher on $\mathcal{CH}$ than is $\mathcal{C}_\alpha$. We claim that ϕ_α^β is Lipschitz with Lipschitz constant $(1-2\alpha)/(1-2\beta)$. To see this, notice that for $x, y \in \mathcal{C}_\beta$ with $x < y$, we know that $|y-x|$ is equal to the sum of the gap lengths contained in the interval $[x, y]$. Since $\phi_\alpha^\beta(x)$ is on the same strand as x and $\phi_\alpha^\beta(y)$ is on the same strand as y, for any stage-n gap $g \subset [x, y]$ of length $|g| = (1-2\beta)\beta^{n-1}$, there is a corresponding stage-n gap $g' \subset [\phi_\alpha^\beta(x), \phi_\alpha^\beta(y)]$ of length $|g'| = (1-2\alpha)\alpha^{n-1}$. Thus

$$\begin{aligned}
|\phi_\alpha^\beta(y) - \phi_\alpha^\beta(y)| &= \sum_n \sum \{|g'| : g' \subset [\phi_\alpha^\beta(x),\ \phi_\alpha^\beta(y)] \text{ is a stage-}n \text{ gap in } \mathcal{C}_\alpha\} \\
&= \sum_n \frac{(1-2\alpha)\alpha^{n-1}}{(1-2\beta)\beta^{n-1}} \sum \{|g| : g \subset [x, y] \text{ is a stage-}n \text{ gap in } \mathcal{C}_\beta\} \\
&\le \frac{1-2\alpha}{1-2\beta}|y-x|.
\end{aligned}$$

In words, ϕ_α^β acts by mapping each gap in $\mathcal{C}_\beta$ to its corresponding gap in $\mathcal{C}_\alpha$; the mapping of the gaps completely defines the action of ϕ_α^β on $\mathcal{C}_\beta$ by "squeezing" each point of $\mathcal{C}_\beta$ between its corresponding gaps. Because of the decay rates for the gap lengths in $\mathcal{C}_\beta$ and $\mathcal{C}_\alpha$, the most stretching is done in mapping the largest gap in $\mathcal{C}_\beta$ to the largest gap in $\mathcal{C}_\alpha$.

We define our desired Lipschitz surjection $\Phi : K_a^b \to \mathcal{C}_a \times [a, b]$ by

$$\Phi(x, y) = (\phi_a^y(x), y).$$

Let $(x_1, y_1), (x_2, y_2) \in K_a^b$ with $y_1 < y_2$. We note that, by construction, $\phi_a^{y_2} = \phi_a^{y_1} \circ \phi_{y_1}^{y_2}$. This suggests that we decompose the action of Φ by first moving (x_2, y_2) to $(\phi_{y_1}^{y_2}(x_2), y_2)$, and then mapping to $(\phi_a^{y_1}(\phi_{y_1}^{y_2}(x_2)), y_2)$. For the point (x_1, y_1), we need only do the one step to $(\phi_a^{y_1}(x_1), x_1)$. By the uniform bound $|\mathcal{T}_\sigma'(y)| \le 2$ (from above), we see that

$$|x_1 - \phi_{y_1}^{y_2}(x_2)| \le |x_1 - x_2| + 2|y_1 - y_2| \le 2(|x_1 - x_2| + |y_1 - y_2|).$$

We know that the mapping $\phi_a^{y_1} : \mathcal{C}_{y_1} \to \mathcal{C}_a$ is Lipschitz, so altogether Φ is also Lipschitz. This proves that $\dim_H(K_a^b) \ge 1 - \ln(2)/\ln(a)$. Taking $a_n = (1/2)(1-1/n)$ and $b_n = (1/2 + a_n)/2$, we see that

$$2 \ge \dim_H(\mathcal{CH}) \ge \dim_H(K_{a_n}^{b_n}) \ge 1 + \frac{\ln(2)}{\ln(2) - \ln\left(\frac{n-1}{n}\right)}, \text{ for all } n > 1,$$

and thus $\dim_H(\mathcal{CH}) = 2$.

By a slight modification of the above procedure, it is possible to construct a Lipschitz surjection $\Psi : K_a^b \to K_c^d$ whenever $c \le a$ and $d \le b$. By this method, we can prove that $\dim_H(K_a^b) = 1 - \ln(2)/\ln(b)$, so the "local" Hausdorff dimension of $\mathcal{CH}$ varies from 1 at $y = 0$ up to 2 at $y = 1/2$.

We can also compute the Hausdorff measure of any K_a^b. For $b = 1/2$, we know that $h^2(\mathcal{CH}) = 0$ and so $h^2(K_a^{1/2}) = 0$ for any $a < 1/2$. Continuing on to $b < 1/2$, let $0 \le a < b < 1/2$ be fixed, $s = \dim_H(K_a^b) = -\ln(2)/\ln(b)$, and $y_n = b - (b-a)/n$ for $n \ge 1$. Then

$$K_a^b = \bigcup_{n \ge 1} K_{y_n}^{y_{n+1}} \cup (\mathcal{C}_b \times \{b\}).$$

Since $\dim_H(K_{y_n}^{y_{n+1}}) < s$ for all n, we know that $h^s(K_{y_n}^{y_{n+1}}) = 0$, and so

$$h^s(K_a^b) \leq \sum_{n\geq 1} h^s(K_{y_n}^{y_{n+1}}) + h^s(\mathcal{C}_b \times \{b\}) = 0.$$

Thus the Hausdorff measures of all the K_a^b are equal to zero, in their dimension.

5.2. The box-counting dimension of $\mathcal{CH}$. The Hausdorff measures have very nice properties but are somewhat difficult to work with. This makes computing the Hausdorff dimension difficult as well. For these, as well as other reasons, many different dimensions and corresponding measures of the "size" of a set have been defined. Among the simplest of these is the *box-counting dimension* (also called the *box dimension*). Given a bounded subset $A \subset \mathbb{R}^d$, let $N_\delta(A)$ be the smallest number of sets of diameter $\delta > 0$ that will cover A. The box-counting dimension measures the asymptotic growth rate of $N_\delta(A)$ as δ decreases to zero, specifically by fitting a model of the form $N_\delta(A) \sim C\delta^{-s}$, and so

$$\dim_B(A) = \lim_{\delta\to 0} \frac{\ln(N_\delta(A))}{-\ln(\delta)}. \tag{15}$$

Of course the limit doesn't have to exist, so in general we have the *upper box dimension* and *lower box dimension* given by

$$\overline{\dim}_B(A) = \limsup_{\delta\to 0} \frac{\ln(N_\delta(A))}{-\ln(\delta)} \quad \text{and} \quad \underline{\dim}_B(A) = \liminf_{\delta\to 0} \frac{\ln(N_\delta(A))}{-\ln(\delta)}.$$

Clearly, for a bounded $A \subset \mathbb{R}^d$ we have $N_\delta(A) = O(\delta^{-d})$, and so $\overline{\dim}_B(A) \leq d$. Furthermore, since $N_\delta(cl(A)) = N_\delta(A)$, we have that the box dimensions of A and $cl(A)$ agree, where $cl(A)$ is the closure of the set A.

Unfortunately, the box dimensions are only finitely stable with $\overline{\dim}_B(\cup_{i=1}^k A_i) = \max_i \overline{\dim}_B(A_i)$. The set $A = \{0\} \cup \{1/n : n \geq 1\} \subset \mathbb{R}$ provides a nice counterexample to countable stability, since $\dim_B(A) = 1/2$, as is easy to show.

We also have a simple relation between the Hausdorff and box-counting dimensions. It is easy to see that $h^s_\delta(A) \leq N_\delta(A)\delta^s$. Thus, if $h^s(A) > 1$, then for sufficiently small $\delta > 0$ we have $0 < \ln(N_\delta(A)) + s\ln(\delta)$, and so $s \leq \underline{\dim}_B(A)$. In particular, for any $s \leq \dim_H(A)$, we have $h^s(A) = +\infty$, and so $s \leq \underline{\dim}_B(A)$. This means that

$$\dim_H(A) \leq \underline{\dim}_B(A) \leq \overline{\dim}_B(A)$$

for any compact A.

Another way to compute the box dimensions will be more useful for us. Given a set $A \subset \mathbb{R}^d$ and $\epsilon > 0$, we define the *ϵ-dilation of A* as

$$A_\epsilon = \{x : d(x, a) < \epsilon, \text{ for some } a \in A\}.$$

Since $\mathcal{L}^d(A_\delta) \leq cN_\delta(A)\delta^d$ for some constant $c > 0$ depending only on d, it's not surprising that there is a relationship between the box dimensions and the decay rate of $\mathcal{L}^d(A_\delta)$, as δ tends to zero. In fact, for $A \subset \mathbb{R}^d$ we have

$$\underline{\dim}_B(A) = d - \limsup_{\delta} \frac{\ln\left(\mathcal{L}^d(A_\delta)\right)}{\ln(\delta)} \tag{16}$$

and

$$\overline{\dim}_B(A) = d - \liminf_{\delta} \frac{\ln\left(\mathcal{L}^d(A_\delta)\right)}{\ln(\delta)}. \tag{17}$$

An especially interesting class of sets is the one composed of the so-called *Minkowski measurable* sets. These are sets $A \subset \mathbb{R}^d$ such that $\lim_{\delta\to 0} \mathcal{L}^d(A_\delta)/\delta^{d-s}$ exists, where $s = \dim_B(A)$. The limit is then called the *Minkowski content* of A. Minkowski measurable sets are analogues of s-sets for box-counting dimension.

Computing the box dimension of K_a^b. The box dimension of $\mathcal{CH}$ is equal to two, since $2 = \dim_H(\mathcal{CH}) \le \underline{\dim}_B(\mathcal{CH}) \le \overline{\dim}_B(\mathcal{CH}) \le 2$. Furthermore, because $\mathcal{CH}_\delta$ decreases to $\mathcal{CH}$ and $\mathcal{L}^2(\mathcal{CH}) = 0$, we know that $\lim_{\delta\to 0} \mathcal{L}^2(\mathcal{CH}_\delta)\delta^{2-2} = 0$, so that $\mathcal{CH}$ is also Minkowski measurable with content equal to zero.

Getting the box dimension of K_a^b is more difficult, and to do this we explicitly estimate the exponential rate of decay in the "tube formula" (which gives the area of $(K_a^b)_\epsilon$). Amazing as it sounds, this is simpler than estimating $N_\delta(K_a^b)$. For the rest of this section we fix $[a, b] \subset [0, 1/2)$ and set $V(\epsilon) = \mathcal{L}^2((K_a^b)_\epsilon)$. We know that

$$1 - \ln(2)/\ln(b) = \dim_H\left(K_a^b\right) \le \underline{\dim}_B\left(K_a^b\right),$$

and thus we just need to get an upper bound on the box dimension.

Our idea is to use an explicit expression for the length, $L_y(\epsilon)$, of the ϵ-dilation of $\mathcal{C}_y$ for each $y \in [a, b]$, and then integrate this over y to get an area. Now, this will give the area of a "horizontal" dilation of K_a^b, and not a true ϵ-dilation of K_a^b. However, if $V(\epsilon)$ is the area of the ϵ-dilation and $V_h(\epsilon)$ is the area of our "horizontal" dilation, then

$$V_h(\epsilon) \le V(\epsilon) \le V_h\left(\sqrt{2}\,\epsilon\right). \tag{18}$$

So if $V_h(\epsilon) \to 0$ as $\epsilon \to 0$, then the same is true for $V(\epsilon)$. For (18), it is important to know that the derivative of any of the functions which parameterize the strands is uniformly bounded by 2. In particular, none of these curves are close to being horizontal. This is also why it is reasonable to integrate the length of the dilation of $\mathcal{C}_y$ and obtain the area of the "horizontal" dilation of K_a^b. That is, for a random stacking of Cantor sets (even with these same interval lengths), there is no reason to expect a geometric relationship between an ϵ-dilation at height y and an ϵ-dilation at a height y'. Since the hairs are analytic functions, there is a smooth change from one $\mathcal{C}_y$ to the nearby $\mathcal{C}_{y'}$, and thus the integration is a reasonable thing to do.

For a given y, $\mathcal{C}_y$ is a central Cantor set with scaling factor y, so from equation (1.9) in [**9**] we see that the length of the ϵ-dilation of C_y is

$$L_y(\epsilon) = 2\epsilon\#\{\text{gaps} \ge 2\epsilon\} + \sum \{\text{all gaps} < 2\epsilon\}. \tag{19}$$

To understand (19), think about the gap endpoints. If x is an endpoint for a gap g and $|g| < 2\epsilon$, then the $g \subset (C_y)_\epsilon$.

As there are 2^n gaps of length $(1-2y)y^n$, then for $(1-2y)y^n \ge 2\epsilon$ we must have

$$n \le N(y, \epsilon) := \left\lfloor \frac{\ln\left(\frac{2\epsilon}{1-2y}\right)}{\ln(y)} \right\rfloor. \tag{20}$$

Thus,

$$L_y(\epsilon) = 2\epsilon(2^{N(y,\epsilon)+1} - 1) + (1 - 2y) \sum_{k>N(y,\epsilon)+1} (2y)^k$$
$$= 2\epsilon(2^{N(y,\epsilon)+1} - 1) + (2y)^{N(y,\epsilon)+2}. \tag{21}$$

We will integrate this expression in y over the range $[a, b]$. The main difficulty is that y influences the value of an integer in both terms. So, we simply break the integral up into parts where this integer value is constant. For each k between $N(a, \epsilon)$ and $N(b, \epsilon)$, let $y_k \in [a, b]$ satisfy $(1 - 2y_k)y_k^k = 2\epsilon$, so that the intervals $[y_k, y_{k+1}]$ form a partition of $[a, b]$. Let $\gamma = 1/(1 - 2b)$. Since $(2\epsilon)^{1/k}$ solves $x^k = 2\epsilon$, we know that

$$(2\epsilon)^{1/k} \le y_k \le (2\epsilon)^{1/k}(1 - 2b)^{-1/k} = (2\epsilon)^{1/k}\gamma^{1/k}.$$

Thus we get

$$\int_a^b L_y(\epsilon)\, dy \le \sum_{k=N(a,\epsilon)}^{k=N(b,\epsilon)} \left\{ 2\epsilon \int_{y_k}^{y_{k+1}} (2^{k+1} - 1)\, dy + \int_{y_k}^{y_{k+1}} (2y)^{k+2}\, dy \right\}$$
$$\le \sum_{k=N(a,\epsilon)}^{k=N(b,\epsilon)} \left\{ 2\epsilon \int_{(2\epsilon)^{1/k}}^{(2\epsilon\gamma)^{1/(k+1)}} (2^{k+1} - 1)\, dy + \int_{(2\epsilon)^{1/k}}^{(2\epsilon\gamma)^{1/(k+1)}} (2y)^k\, dy \right\}. \tag{22}$$

First, estimate the second integral in (22) and its contribution to the sum. We see that

$$\int_{(2\epsilon)^{1/k}}^{(2\epsilon\gamma)^{1/(k+1)}} (2y)^k\, dy = 2\epsilon \frac{2^k}{k+1} \left(\gamma - (2\epsilon)^{1/k}\right) \le 2\epsilon\gamma \frac{2^k}{k+1}.$$

Thus we have that the integral of the second term goes as

$$2\epsilon\gamma \sum_{k=N(a,\epsilon)}^{k=N(b,\epsilon)} \frac{2^k}{k+1} \sim 2\epsilon\gamma \int_{N(a,\epsilon)}^{N(b,\epsilon)} \frac{2^x}{x+1}\, dx$$
$$\sim 2\epsilon\gamma \left(2^{N(b,\epsilon)}\right) \left(\frac{1}{\ln(2) N(b, \epsilon)} + \text{H.O.T.} \right)$$
$$\sim (2\epsilon)^{1+\ln(2)/\ln(b)} \frac{C}{|\ln(2\epsilon) - \ln(1 - 2b)|}. \tag{23}$$

Estimating the first term in (22) is similar. Using the Mean Value Theorem for the function $(x, y) \mapsto x^{1/y}$, we have

$$\int_{(2\epsilon)^{1/k}}^{(2\epsilon\gamma)^{1/(k+1)}} \left(2^{k+1} - 1\right)\, dy = \left(2^{k+1} - 1\right) \left((2\epsilon\gamma)^{1/(k+1)} - (2\epsilon)^{1/k}\right)$$
$$\le 2^{k+1}(2\epsilon\gamma)^{1/(k+1)} \left(\frac{\gamma - 1}{k} - \frac{\ln(2\epsilon)}{k^2} \right).$$

Thus,

$$2\epsilon \sum_{k=N(a,\epsilon)}^{k=N(b,\epsilon)} \int_{(2\epsilon)^{1/k}}^{(2\epsilon\gamma)^{1/(k+1)}} \left(2^{k+1}-1\right) dy$$

$$\leq 4\epsilon\gamma \left[(\gamma-1) \sum_{k=N(a,\epsilon)}^{k=N(b,\epsilon)} \frac{2^k}{k} - \ln(2\epsilon) \sum_{k=N(a,\epsilon)}^{k=N(b,\epsilon)} \frac{2^k}{k^2} \right]. \tag{24}$$

The first sum has the same estimate as (23). For the second sum, we see that

$$\int_{N(a,\epsilon)}^{N(b,\epsilon)} \frac{2^x}{x^2}\, dx \sim 2^x \frac{1}{\ln(2) N(b,\epsilon)^2}.$$

Putting this information together, we obtain

$$2\epsilon \sum_{k=N(a,\epsilon)}^{k=N(b,\epsilon)} \int_{(2\epsilon)^{1/k}}^{(2\epsilon\gamma)^{1/(k+1)}} \left(2^k - 1\right) dy = O\left((2\epsilon)^{1+\ln(2)/\ln(b)} \frac{C}{|\ln(2\epsilon) - \ln(1-2b)|} \right). \tag{25}$$

The final result of (23) and (25) is that

$$V(\epsilon)/\epsilon^{1+\ln(2)/\ln(b)} = O\left(\frac{1}{\ln(2\epsilon)}\right).$$

So $\dim_B(K_a^b) = 2 - [1 + \ln(2)/\ln(b)] = 1 - \ln(2)/\ln(b)$. Furthermore, K_a^b is Minkowski measurable with content equal to zero, because of the $\ln(2\epsilon)$ in the denominator of both (23) and (25). Note, however, that the decay to zero is very slow.

Comments. We notice that $\dim_H(\mathcal{CH}) = 2$, but that $\mathcal{L}^2(\mathcal{CH}) = 0 = h^2(\mathcal{CH})$, and so $\mathcal{CH}$ is a rather simple example of a set with maximal dimension and zero measure. It is a more interesting and simpler example of this than the set

$$S = \left\{ x \in [0,1] : \lim_n \frac{\#\{1 \leq i \leq n : i\text{th binary digit of } x \text{ is one}\}}{n} \text{ does not exist} \right\},$$

which is a 1-dimensional set with zero Lebesgue measure. However, S is not compact and $cl(S) = [0,1]$, so the Minkowski content doesn't agree with the Lebesgue measure, unlike in the case of $\mathcal{CH}$. The behaviour of $\mathcal{CH}$ and K_a^b is the same with respect to both the Hausdorff and box-counting dimensions and with respect to the Hausdorff measure and Minkowski content.

6. GENERALIZATIONS. It is pretty simple to change the construction of $\mathcal{CH}$ to obtain variations, such as the sets illustrated in Figure 2.

The idea is to vary the "stack" of Cantor sets. This is accomplished by changing the contraction factor for the maps in (4) from y to some function $g(y)$ of y. That is, we use the two maps

$$w_0(x,y) = g(y)\,x \quad \text{and} \quad w_1(x,y) = g(y)\,x + (1 - g(y)), \tag{26}$$

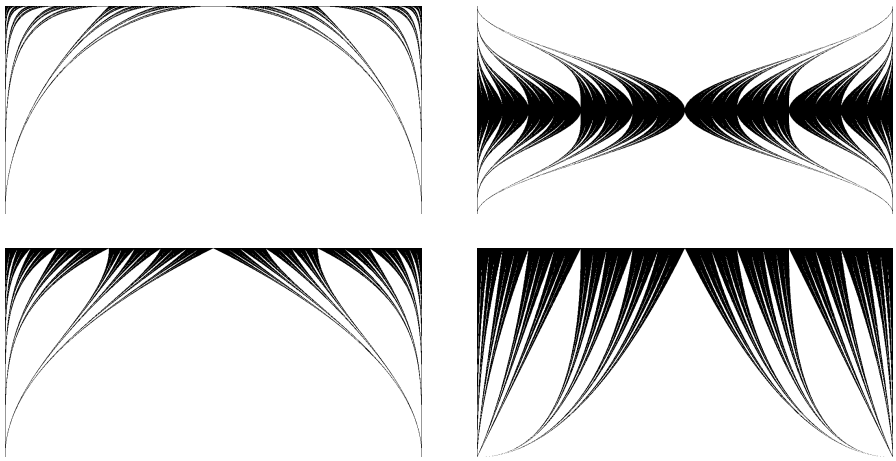

Figure 2. Variations on $\mathcal{CH}$

for some appropriate (and interesting) choice for $g(y)$. Figure 2 illustrates (clockwise from upper left) the sets associated with the functions $g(y) = 1/2 - \sqrt{1/4 - y^2}$, $g(y) = \sin(2\pi y)/2$, and $g(y) = \sqrt{y/2}$, $g(y) = 2y^2$. The only real restriction on g is that $0 \le g(y) \le 1/2$ for $y \in [0, 1/2]$. For polynomial g, it is easy to do explicit computations. We see that, just as in the standard case of $g(y) = y$, all the visible strands in the image are polynomial functions of y.

We will use $\mathcal{CH}_g$ to denote the version of $\mathcal{CH}$ associated with the function $g(y)$.

Area of "gaps." For particular choices of $g(y)$ it is also possible to obtain explicit values for the areas of the "gaps" in $\mathcal{CH}_g$. One non-polynomial case, where we set $g(y) = 1/2 - \sqrt{1/4 - y^2}$, is particularly interesting. In this case, the central gap is a semi-circle. The calculations in this case are more complicated than in the standard case, but it is still relatively simple to obtain explicit formulas for the areas of the "gaps." The formula for the area of an nth stage "gap" is

$$2^{-n-1} \int_0^{1/2} \sqrt{1 - 4y^2} \left(1 - \sqrt{1 - 4y^2}\right)^{n-1} dy.$$

This is a perfect integral for a trigonometric substitution of the form $y = \sin(\theta)/2$, giving the integral

$$A_n = 2^{-n-2} \int_0^{\pi/2} \cos^2(\theta)(1 - \cos(\theta))^{n-1} \, d\theta.$$

Explicitly computing these and checking to see if they sum to $1/2$ is rather tedious. A nice trick, however, is to see that the total area is equal to

$$\begin{aligned} \sum_n 2^n A_n &= \frac{1}{2} \int_0^{\pi/2} \cos^2(\theta) \sum_{n \ge 0} (1 - \cos(\theta))^n \, d\theta \\ &= \frac{1}{2} \int_0^{\pi/2} \cos^2(\theta) \frac{1}{1 - 1 + \cos(\theta)} \, d\theta \\ &= \frac{1}{2} \int_0^{\pi/2} \cos(\theta) \, d\theta = \frac{1}{2}. \end{aligned}$$

We leave it up to the reader to justify the exchange of the infinite sum and the integral. This calculation is part of a more general fact. For a general function $g(y)$, we have that the Cantor set at "level" y with scaling ratio $g(y)$ has Lebesgue measure zero (as long as $g(y) < 1/2$), since the sum of the gaps is

$$\sum_{n\geq 1}(1-2g(y))(g(y))^{n-1} = \frac{1-2g(y)}{1-2g(y)} = 1.$$

The area of one of the 2^{n-1} nth "stage" gaps is

$$\int_0^{1/2}(1-2g(y))(g(y))^{n-1}\,dy,$$

and so the sum of all of them is

$$\begin{aligned}\sum_{n\geq 1}\int_0^{1/2}(1-2g(y))(g(y))^{n-1}\,dy &= \int_0^{1/2}\sum_{n\geq 1}(1-2g(y))(g(y))^{n-1}\,dy \\ &= \int_0^{1/2} 1\,dy = \frac{1}{2}.\end{aligned}$$

Thread functions are real-analytic. If the function $g(y)$ is real-analytic, then so are all the thread functions. This is rather simple to show, since in this case the thread function for $\sigma \in \Sigma$ is given by

$$\mathcal{T}_\sigma^g(y) = (1-g(y))g(y)^{-1}\sum_{n\geq 1}\sigma_n g(y)^n, \tag{27}$$

for all y such that $g(y) \neq 0, 1$. In fact, we see that $\mathcal{T}_\sigma^g = \mathcal{T}_\sigma \circ g$, and so $\mathcal{T}_\sigma^g$ is real-analytic, as it is the composition of two real-analytic functions. From this viewpoint, the standard version of $\mathcal{CH}$ has a "universality" property, since the thread functions for any variation are constructed in a simple way from the thread functions of the standard version.

Geometric measure-theoretic properties. Suppose that both g and g^{-1} are C^1. Then the following function $\Phi : \mathcal{CH} \to \mathcal{CH}_g$ is easily seen to be bi-Lipschitz:

$$\Phi(x, y) = (x, g^{-1}(y)).$$

Thus $dim_H(\mathcal{CH}_g) = 2$ and $\mathcal{L}^2(\mathcal{CH}_g) = h^2(\mathcal{CH}_g) = 0$ under these conditions. Notice that this condition is satisfied for three of the examples in Figure 2.

Furthermore, under this same condition the integral estimates for the "horizontal" tube formula for $\mathcal{CH}_g$ are a straightfoward change-of-variable from that for $\mathcal{CH}$, so we obtain the same decay rate, up to a constant multiplier.

Since we obtained the Hausdorff dimension, Hausdorff measure, box dimension, and Minkowski content for K_a^b for any $0 \leq a < b \leq 1/2$, we can use this information to analyze these same local properties of any $\mathcal{CH}_g$.

ACKNOWLEDGMENTS. The second author was partially supported by a Discovery Grant from the Natural Sciences and Engineering Research Council of Canada.

1. M. F. Barnsley, *Fractals Everywhere*, Academic Press, New York, 1988.
2. C. Cabrelli, F. Mendivil, U. Molter, R. Shonkwiler, On the Hausdorff h-measure of Cantor sets, *Pac. J. Math.* **217** (2004) 45–59, available at http://dx.doi.org/10.2140/pjm.2004.217.45.
3. K. J. Falconer, *Fractal Geometry–Mathematical Foundations and Applications*, second edition, Wiley, New York, 2003.
4. ———, *Techniques in Fractal Geometry*, Wiley, New York, 1997.
5. J. A. Guthrie, J. E. Nymann, The topological structure of the set of subsums of an infinite series, *Colloq. Math.* **55** (1988) 323–327.
6. K. Hannabus, Mathematics in Victorian Oxford: A Tale of Three Professors, in *Mathematics in Victorian Britain*, Edited by R. Flood, A. Rice, R. Wilson, Oxford University Press, Oxford, 2011. 35–52.
7. J. E. Hutchinson, Fractals and self-similarity, *Indiana Univ. J. Math.* **30** (1981) 713–747, available at http://dx.doi.org/10.1512/iumj.1981.30.30055.
8. S. Kakeya, On the partial sums of an infinite series, *Tohoku Sci. Rep.* **3** no. 4 (1914) 159–164.
9. M. L. Lapidus, M. Van Frankenhuijsen, *Fractal Geometry, Complex Dimensions and Zeta Functions: Geometry and Spectra of Fractal Strings*, Springer, New York, 2006.
10. B. Mandelbrot, *The Fractal Geometry of Nature*, W. H. Freeman, New York, 1983.
11. P. K. Menon, On a class of perfect sets, *Bull. Amer. Math. Soc.* **54** (1948) 706–711, available at http://dx.doi.org/10.1090/S0002-9904-1948-09060-7.
12. C. A. Rogers, *Hausdorff Measures*, reprint of the 1970 original, Cambridge University Press, Cambridge, 1998.
13. S. G. Krantz, H. R. Parks, *The Geometry of Domains in Space*, Birkhäuser, Boston, 1999.

JACQUES LÉVY VÉHEL is a research director at Inria in France. He is interested in understanding irregularity in natural phenomena, using tools in harmonic analysis, probability theory, and fractal analysis.
Regularity team, INRIA Saclay and MAS Laboratory, Ecole Centrale Paris, Grande Voie des Vignes, 92295 Chatenay-Malabry Cedex, France
jacques.levy-vehel@inria.fr

FRANKLIN MENDIVIL is a professor of mathematics at Acadia University in Nova Scotia. His research is a blend of fractal geometry and analysis, image processing, and optimization. He considers himself extremely lucky to be in a profession that allows him to explore many different topics.
Department of Mathematics and Statistics, Acadia University, 12 University Avenue, Wolfville, NS Canada B4P 2R6
franklin.mendivil@acadiau.ca

Growth Rate of Calculus Textbooks

When students express surprise that there is anything new in mathematics, I point them to this table of calculus book page counts. The growth rate is 0.7% per year and increasing (not to mention that pages are getting larger). Based on this, we can safely predict a 2000 page calculus book by the year 2090.

Year	Author	Pages
1716	L'Hôpital	202
1836	Davies	286
1937	Courant	661
1993	Thomas/Finney 2nd	1094
2011	Stewart 7th	1368

—Submitted by Vadim Ponomarenko

http://dx.doi.org/10.4169/amer.math.monthly.120.09.786
MSC: Primary 26-01, Secondary 26A06